Research Report

LncRNA HEIH/miR-4500/IGF2BP1/c-Myc Feedback Loop Accelerates Bladder Cancer Cell Growth and Stemness

Baowei Guo[a,*], Dan Zhao[a], Jiao Feng[b] and Yanmei Liu[c]
[a]*Department of Urology, Yidu Central Hospital of Weifang, Qingzhou City, Weifang, Shandong, China*
[b]*Department of Ophthalmology, Yidu Central Hospital of Weifang, Weifang, Shandong, China*
[c]*Clinical Laboratory, Yidu Central Hospital of Weifang, Weifang, Shandong, China*

Abstract.
BACKGROUND: Bladder cancer (BCa) is one of the most prevalent malignancies and more common in men. An aberrantly expressed long noncoding RNA (lncRNA) hepatocellular carcinoma up-regulated EZH2-associated lncRNA (HEIH) has been reported to be implicated in the progression of many cancers, but its role in BCa remains little known. Our study intended to uncover whether and how HEIH regulates BCa progression.
MATERIALS AND METHODS: Quantitative real-time polymerase chain reaction (RT-qPCR) was adopted to determine HEIH expression in BCa cell lines. Functional experiments were performed to examine the effects of HEIH on BCa cell proliferation, apoptosis, migration, invasion and stemness. Bioinformatics analysis and mechanism experiments were conducted to investigate the regulatory relationship between HEIH and related molecules in BCa.
RESULTS: HEIH expression was observed to be significantly increased in BCa cell lines. HEIH depletion significantly hindered BCa cell proliferation, migration and invasion. Besides, HEIH up-regulated MYC proto-oncogene, and bHLH transcription factor (c-Myc) expression to promote BCa cell stemness. Moreover, HEIH served as a sponge for miR-4500 to modulate insulin-like growth factor 2 mRNA binding protein 1 (IGF2BP1) expression, thereby stabilizing c-Myc mRNA level.
CONCLUSION: Our study demonstrated a positive feedback loop of HEIH/miR-4500/IGF2BP1/c-Myc in BCa progression, offering a novel insight into a possible BCa therapy.

Keywords: Bladder cancer, HEIH, IGF2BP1, c-Myc

INTRODUCTION

Bladder cancer (BCa) is the most common malignant urinary tumor [1]. The incidence of BCa has gradually increased in recent years [2]. Although great improvements have been made in therapeutic strategies, including surgery, chemotherapy and immunotherapy, the prognosis of patients with BCa is

*Correspondence to: Baowei Guo, Department of Urology, Yidu Central Hospital of Weifang, No.4138 Linglongshan South Road, Qingzhou City, Weifang, 262500, Shandong, China. E-mail: guobw@163.com.

still unsatisfactory [3]. A great number of researches have deepened our understanding of the pathogenesis of BCa, but the molecular mechanisms underlying this malignant disease remain poorly understood [4]. Hence, it is of great necessity to explore the molecular mechanism governing BCa and explore potential targets for BCa treatment.

Cancer stem cells (CSCs), also named as tumor-initiating cells, are a class of tumor cells with self-renewal and limitless replication capacities so as to induce the carcinogenesis of multiple cancers, including BCa [5, 6]. Thus, assessment of the molecular mechanisms underlying CSCs is required.

With advanced RNA sequencing techniques, over 90% of DNA sequences can be transcribed into RNAs, but only less than 2% of these transcripts have protein-encoding capacity, while the majority of transcripts are noncoding RNAs (ncRNAs) [7]. LncRNAs are a class of RNA molecules which possess a length of exceeding 200 nucleotides [8]. LncRNAs involve in the progression of cancers by regulating gene expression at epigenetic, transcriptional and post-transcriptional levels [9]. The mushroom growth of RNA genomics has emphasized the potential of lncRNAs in a variety of human cancers, and BCa is no exception [10]. Remarkably, lncRNAs serve as oncogenes or tumor repressors to regulate BCa cell proliferation, migration and invasion [11, 12].

Previous studies have suggested that HEIH participates in the progression of various cancers [13, 14]. For instance, HEIH functions as an oncogene in breast cancer [15]. HEIH accelerates cell migration and invasion in cholangiocarcinoma via regulating the miR-98-5p/HECTD4 axis [16]. HEIH contributes to ovarian cancer cell proliferation by regulating the miR-3619-5p/CTTNBP2 axis [17]. Nonetheless, the role of HEIH in BCa remains largely obscure.

According to GEPIA analysis, HEIH was markedly over-expressed in BCa tissues versus normal tissues. Given that, we wondered whether up-regulation of HEIH is implicated in BCa development. At the same time, the molecular mechanism by which HEIH elicits its function in BCa cells was also investigated in this study.

MATERIALS AND METHODS

Cell culture

The immortalized human bladder epithelium cell line SV-HUC-1 (CRL-9520, ATCC; Manassas, VA) was grown in Ham's F-12K Medium. Human BCa cell lines were all procured from ATCC and maintained in various culture media. T24 cell line (HTB-4) was maintained in Dulbecco's Modified Eagle Medium (DMEM), 5637 cell line (HTB-9) in RPMI-1640, J82 cell line (HTB-1) in Minimum Essential Medium (MEM) and RT-4 cell line (HTB-2) in McCoy's 5A. All media were treated with 10% fetal bovine serum (Gibco, USA) and cultured at $37°C$ with 5% CO_2. All the above cell lines have been recently tested for no contamination and have been authenticated using short tandem repeat (STR) analysis.

Mouse xenograft model

Nude mice commercially procured from the Model Animal Research Center of Nanjing University were kept under laboratory conditions. Animal study was approved by the Yidu Central Hospital of Weifang (NO. YD-21-037). Stable T24 cells expressing sh-HEIH#1, or sh-NC were subcutaneously injected into nude mice ($5 × 10^6$ cells per mouse). Tumor volume was measured and recorded every three days. 27 days later, tumors and lung tissues were excised after mice were subjected to anesthesia. The xenografted tumors were weighed. Lung metastatic nodules were photographed after haematoxylin and eosin (H&E) staining (Beyotime, Shanghai, China). Then, the number of lung metastatic nodules was counted.

RT-qPCR

Total RNAs were extracted from RT-4, T24, 5637 and J82 cell lines (SV-HUC-1 as control) or transfected BCa cells (T24 and J82) employing Trizol kit (Invitrogen, Carlsbad, CA) for reverse-transcription with PrimeScript RT Reagent Kit (Takara, Otsu, Japan). RNA expression was detected by qPCR using SYBR Green PCR Master Mix (Takara) and calculated by $2^{-\Delta\Delta CT}$ method, normalized to GAPDH or U6. This assay was independently repeated 3 times. The sequences of primers used in the current study were reported in Table 1.

Plasmids and transfection

The interference sequences were designed based on the sequence of HEIH, IGF2BP1 or c-Myc (two interference sequences for each). Then, interference sequences were inserted into interference vector to generate sh-HEIH#1/2, sh-IGF2BP1#1/2 or sh-c-Myc#1/2. In this study, the specific short hairpin

Table 1
Primer sequences

Primer	Sequence
HEIH-F	AGGTCATCTGATCACGTCGC
HEIH-R	TTGCGTAGAGGTAGCTGGGT
c-Myc-F	CGTCCTCGGATTCTCTGCTC
c-Myc-R	GCTGCGTAGTTGTGCTGATG
miR-2467-3p-F	GCCGAGagcagaggcagagagg
miR-2467-3p-R	CTCAACTGGTGTCGTGGA
miR-4458-F	GCCGAG agaggtaggtgtg
miR-4558-R	CTCAACTGGTGTCGTGGA
miR-4500-F	GCCGAG tgaggtagtag
miR-4500-R	CTCAACTGGTGTCGTGGA
let-7a-5p-F	GCCGAGtgaggtagtaggttgt
let-7a-5p-R	CTCAACTGGTGTCGTGGA
let-7b-5p-F	GCCGAG tgaggtagtaggttgt
let-7b-5p-R	CTCAACTGGTGTCGTGGA
let-7c-5p-F	GCCGAG tgaggtagtaggttgt
let-7c-5p-R	CTCAACTGGTGTCGTGGA
let-7d-5p-F	GCCGAG agaggtagtaggttgc
let-7d-5p-R	CTCAACTGGTGTCGTGGA
let-7e-5p-F	GCCGAG tgaggtaggaggttgt
let-7e-5p-R	CTCAACTGGTGTCGTGGA
let-7f-5p-F	GCCGAG tgaggtagtagattgt
let-7f-5p-R	CTCAACTGGTGTCGTGGA
miR-98-5p-F	GCCGAG tgaggtagtaagttgt
miR-98-5p-R	CTCAACTGGTGTCGTGGA
let-7g-5p-F	GCCGAG tgaggtagtagtttgt
let-7g-5p-R	CTCAACTGGTGTCGTGGA
let-7i-5p-F	GCCGAG tgaggtagtagtttgt
let-7i-5p-R	CTCAACTGGTGTCGTGGA
miR-193a-5p-F	GCCGAG tgggtctttgcgggcg
miR-193a-5p-R	CTCAACTGGTGTCGTGGA
CNIH4-F	CGCTCATCTTCCTCTCGGTC
CNIH4-R	GACTTCAGCTGCCCTCGATT
LRRC23-F	GCTGATTTGCGCATCAGGTAG
LRRC23-R	AAGGAGGGGTTGTGTACTGC
DICER1-F	GATGGTTCTCGAAGGCCCG
DICER1-R	ACCCATTGGTGAGGAAGCAG
GGA3-F	CAATATGGCGGAGGCGGAAG
GGA3-R	TTCCTGTGGGGACTGGATCT
IGF2BP1-F	CTCCTTTATGCAGGCTCCCG
IGF2BP1-R	GGGTCTCCAGCTTCACTTCC
PSME4-F	CCAGTGGGAAGCAGTCAAGT
PSME4-R	TTGGCAACCGCTGAAGTAGT
ZNF142-F	CCTGTCTCCTACCTCACCCT
ZNF142-R	GGCACAGTCCATCCATCTCC
FNIP2-F	GGAAGGACCCGCCTTTAGTT
FNIP2-R	CCCCAGAAGAACTGTGGGAA
ASAP1-F	GATTCTCAGAGCCGGCAAGG
ASAP1-R	CCGGATCCGTCACTTTTCT
GAPDH-F	CTCTGCTCCTCCTGTTCGAC
GAPDH-R	TTCCCGTTCTCAGCCTTGAC
U6-F	TCCCTTCGGGGACATCCG
U6-R	AATTTTGGACCATTTCTCGATTTGT

F: forward primer; R: reverse primer.

RNAs (shRNAs) and negative controls (sh-NCs) were constructed by Genechem (Shanghai, China) to silence HEIH, IGF2BP1 or c-Myc expression, along with the control pcDNA3.1 and pcDNA3.1/c-Myc to overexpress c-Myc expression. Besides, miR-4500

mimics and NC mimics, miR-4500 inhibitor and NC inhibitor were procured from Genepharma Company (Shanghai, China). Lipofectamine 3000 (Invitrogen) was utilized for plasmid transfection for 48 h. All assays were independently repeated 3 times.

Colony formation assay

T24 and J82 cells were seeded post transfection at a density of 500 cells/well to the 6-well plates. Subsequent to 14 days of incubation, colonies were fixed, stained, and counted. All assays were independently repeated thrice.

5-ethynyl-2'-deoxyuridine (EdU) assay

T24 and J82 cells post transfection were placed to a 96-well plate. EdU assay kit (RiboBio, Guangzhou, China) was used as instructed by the supplier. The nucleus was labeled by DAPI. Images were acquired using a fluorescent microscope (Leica, Wetzlar, Germany). All assays were independently repeated 3 times.

Flow cytometry analysis

Annexin-V fluorescein isothiocyanate (FITC)/ propidium iodide (PI) dual staining kit was commercially available from BD Biosciences (San Jose, CA) to perform flow cytometry analysis as guided by the manufacturer. Apoptosis of BCa cells were examined by FACSCalibur™ Flow Cytometer (BD Bioscience). All assays were independently conducted 3 times.

JC-1 assay

This assay was performed by assessing the changes in mitochondrial transmembrane potential ($\Delta\Psi$m). Cells in 96-well plates were centrifuged for loading with JC-1 dye for 30 min. All assays were independently repeated 3 times.

Transwell assay

Transfected T24 and J82 cells (1×10^4) were seeded onto the upper transwell chamber (8-μm pore; Corning Incorporated, Corning, NY), with lower chamber filled with complete medium. After 24 h, cells were fixed and stained. Images were captured in 5 randomly selected fields using microscope. For invasion assay, membranes were pre-coated with

Matrigel (Millipore, Billerica, MA). All assays were independently repeated 3 times.

Sphere formation assay

Transfected cells were plated on ultra-low attachment plates (Corning) in serum-free medium supplemented with 20 ng/mL EGF, 20 ng/mL FGF, 4 mg/mL heparin and 2% B27 for 2 weeks, the sphere number and size were analyzed. All assays were independently repeated 3 times.

Western blot

Total proteins extracted from RT-4, T24, 5637 and J82 cell lines (SV-HUC-1 as control) or transfected BCa cells (T24 and J82) were transferred to PVDF membranes after separation with 12% sodium dodecyl sulfate polyacrylamide gel electrophoresis (SDS-PAGE). The membranes were then blocked and incubated with the primary antibody. The antibodies used in this study include anti-Nanog (Abcam, 1/1000), anti-OCT4 (Abcam, 1/1000), anti-KLF4 (Abcam, 1/1000), anti-SOX2 (Abcam, 1/1000), anti-c-Myc (Abcam, 1/1000), anti-IGF2BP1 (Abcam, 1/1000) and anti-GAPDH (Abcam, 1/1000). Next, the membranes were treated with secondary antibodies and detected with enhanced chemiluminescence (ECL) using a BeyoECL Plus Kit (Beyotime). All assays were independently repeated 3 times.

Immunohistochemical (IHC) analysis

Tissues excised from experimental mice were fixed in 10% formalin at 4°C overnight and embedded in paraffin. Afterwards, the paraffin sections (4-μm thick) were permeabilized with 0.5% Triton X-100 in PBS for 1 h, followed by the incubation with specific primary antibodies (anti-PCNA, Abcam, 1/1000) at 4°C overnight. Subsequent to PBS washes 3 times, HRP-conjugated secondary antibodies were added. Slides were photographed by a confocal microscope.

Fluorescent in situ hybridization (FISH)

HEIH-FISH probe was produced by RiboBio for FISH assay following the manufacturer's instructions. Cell nucleus was processed with Hoechst reagent, and then stained cells were analyzed by fluorescent microscope. All assays were independently repeated 3 times.

Subcellular fractionation

The processed cells (1×10^7) were suspended in cell fraction buffer, and incubated on ice to acquire cytoplasmic fraction. After the addition of cell disruption buffer, the nuclear fraction was obtained. HEIH expression in the isolated nuclear and cytoplasmic fractions of T24 and J82 cells were measured. All assays were independently repeated 3 times.

RNA-binding protein immunoprecipitation (RIP)

This assay was performed in cells using Magna RNA-binding protein immunoprecipitation kit (Millipore) based on the supplier's suggestions. Transfected cells were lysed in lysis buffer. Cell lysates were collected and immunoprecipitated with human antibody against Argonaute 2 (anti-Ago2), IGF2BP1 (anti-IGF2BP1) or negative control immunoglobulin G (anti-IgG) antibody overnight at 4°C. Magnetic beads were conjugated with antibodies for collecting precipitates. RNA extraction and RT-qPCR analysis were followed. All assays were independently repeated 3 times.

RNA pull down assay

This experiment was conducted by means of the Pierce™ Magnetic RNA-Protein Pull-Down Kit (Thermo Fisher Scientific, Waltham, MA) following the manufacturer's user guide. Cell lysates were used to mix with biotinylated RNA probes and beads. The relative enrichment of RNA was assayed. All assays were independently repeated 3 times.

Chromatin immunoprecipitation (ChIP)

A ChIP assay kit (Beyotime, China) was employed in this experiment as per the supplier's protocols. T24 and J82 cells were cross-linked and sonicated to shear DNA to 200 and 1,000 base pairs in length. Cell lysates were incubated with protein A/G beads coated with the anti-c-Myc antibody. Anti-IgG was used as a negative control. After immunoprecipitation, the bound DNA fragments were purified and subjected to RT-qPCR. All assays were independently repeated 3 times.

Luciferase reporter assay

The sequence of HEIH or IGF2BP1 3'UTR fragments covering the wild-type and mutated miR-4500

binding sites was sub-cloned into the downstream of pmirGLO luciferase vectors (Promega, Madison, WI). The established HEIH-WT/Mut and IGF2BP1 3'UTR-WT/Mut reporter vectors were co-incubated with miR-4500 mimics or NC mimics in T24 and J82 cells. To determine the impacts of c-Myc on HEIH promoter, transfected T24 and J82 cells were treated with the pGL3-based construct containing HEIH WT or Mut promoter sequences for 48 h. Luciferase activities of firefly and Renilla luciferases were both monitored by Luciferase Reporter Assay System (Promega). Each assay was independently conducted 3 times.

RNA stability analysis

T24 cells were transfected with sh-IGF2BP1#1/2 using Lipofectamine 3000. Then, 2 mg/ml Actinomycin D (a transcriptional inhibitor; Shanghai PureOne Biotechnology, Shanghai, China) was added to interfere with RNA synthesis. Transfected T24 cells treated with Actinomycin D were harvested at different time points (0, 2, 4, 6, 8 h), followed by RNA isolation. Expression level of c-Myc was detected via RT-qPCR.

Statistical analyses

Statistical analysis was conducted by the application of GraphPad Prism 7.0 Software (GraphPad Software, La Jolla, CA). All assays were conducted 3 times, and the data were expressed as the mean $\pm$ standard deviation (SD). The significance of group difference was examined by Student's *t*-test and one-way/two-way ANOVA. A threshold was defined as 0.05 (typically $P < 0.05$) to indicate statistical significance.

RESULTS

Expression and function of HEIH in BCa

To identify potential lncRNAs associated with the pathogenesis of BCa, we firstly adopted the GEPIA analysis and discovered that lncRNA HEIH was highly expressed in BCa tissue samples versus normal tissues ($P < 0.05$; Fig. 1A). Then, we also detected relatively higher expression of HEIH in BCa cell lines compared with human normal bladder epithelial cell line SV-HUC-1 (Fig. 1B). To discuss the effect of HEIH on BCa tumorigenesis, T24 and J82 cells which exhibited the highest expression of HEIH were transfected with shRNAs against HEIH (sh-HEIH#1/2; Fig. 1C). The results followed by colony formation and EdU experiments showed that HEIH deficiency significantly inhibited BCa cell proliferation (Fig. 1D-1E). Besides, flow cytometry analysis and JC-1 assay demonstrated that the percentage of apoptotic cells was increased by HEIH depletion (Fig. 1F-1G). By performing transwell assays, we examined the influence of HEIH silence on the migratory and invasive capacities of BCa cells. The number of migrated and invaded cells in HEIH-silenced group was lower than the control group (Fig. 1H-1I). Collectively, these data showed the upregulation of HEIH expression in BCa cell lines and manifested that the deficiency of HEIH hampers cell proliferation, migration and invasion but promotes cell apoptosis in BCa.

HEIH contributes to BCa cell stemness via up-regulating c-Myc

Since CSC properties exert important roles in the progression of human cancers [5], we assessed the effects of HEIH on CSC characteristics. Sphere formation assay illustrated HEIH inhibition reduced the size of sphere and sphere formation efficiency (Fig. 2A). It is well known that Nanog, OCT4, KLF4, SOX2 and c-Myc are major regulators involved in cancer cell stemness. Next, we investigated whether HEIH contributes to BCa cell stemness by regulating some of these CSC-associated genes. Through western blot, we found that HEIH knockdown only decreased the protein level of c-Myc, while barely affected the level of other proteins (Fig. 2B). RT-qPCR analysis further validated that HEIH positively regulates c-Myc expression in terms of mRNA level (Fig. 2C). Further, the analysis of GEPIA database displayed the correlation between Myc and HEIH in bladder urothelial carcinoma (BLCA) (Fig. 2D). Collectively, HEIH facilitates BCa cell stemness via up-regulating c-Myc.

HEIH functions as a miR-4500 sponge in BCa cells

In addition to its biological role, we explored the regulatory mechanism of HEIH in BCa. Firstly, the distribution of HEIH was determined by FISH and nucleus/cytoplasm fractionation assays. The analysis of subcellular localization revealed that HEIH was
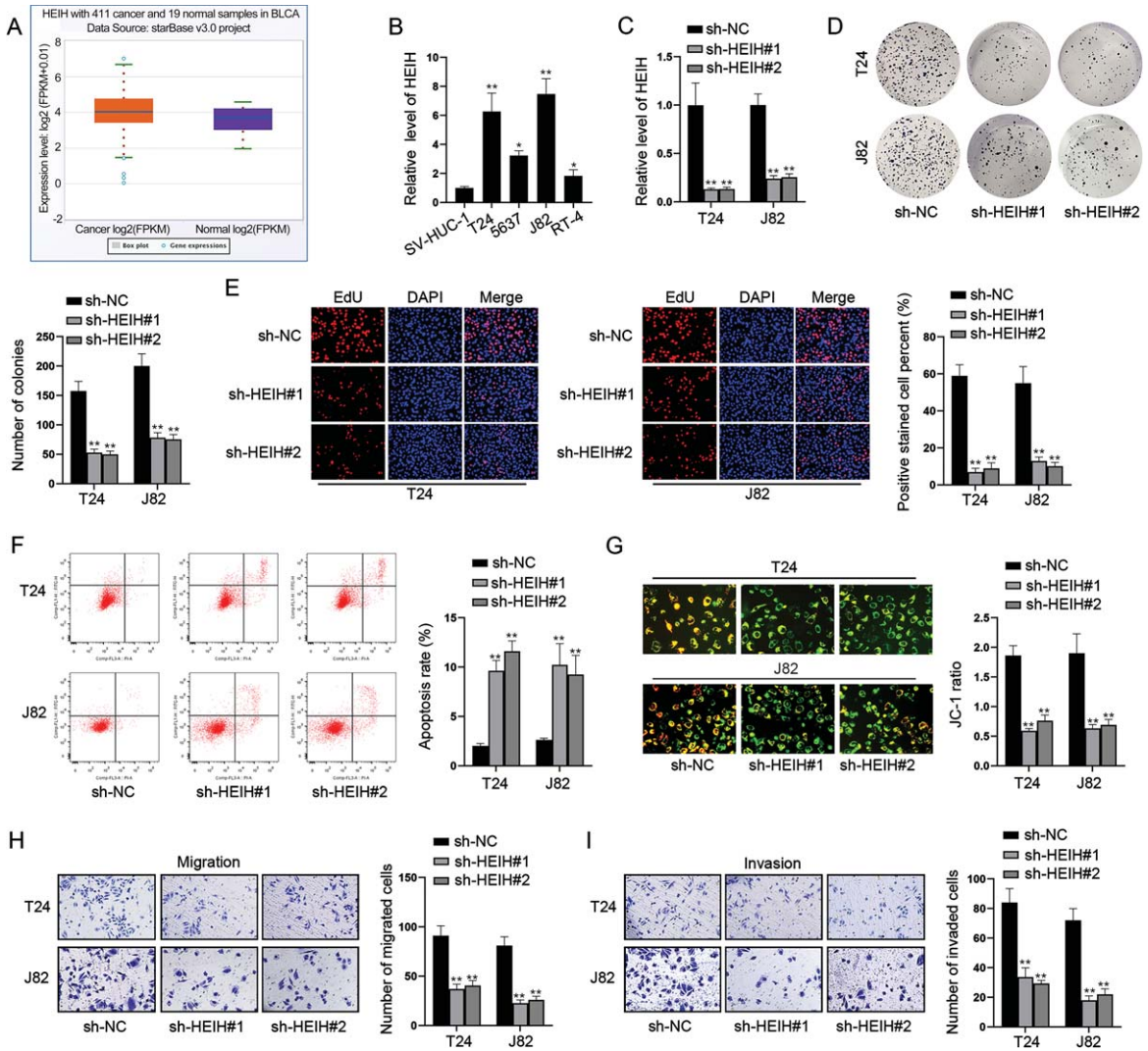
Fig. 1. HEIH silence inhibits BCa cell proliferation, migration and invasion. (A) HEIH expression in BCa tissue samples ($n = 411$) and normal samples ($n = 19$) from TCGA database ($P < 0.05$). (B) HEIH expression in BCa cell lines was examined by RT-qPCR. (C) The interference efficiency of sh-HEIH was detected by RT-qPCR. (D-E) Colony formation and EdU experiments were performed to test BCa cell proliferation after HEIH silence. (F-G) Flow cytometry analysis and JC-1 experiment were conducted to estimate BCa cell apoptosis after HEIH knockdown. (H-I) Transwell migration and invasion assays were carried out to evaluate BCa cell migration and invasion after the ablation of HEIH. $^*P < 0.05$, $^{**}P < 0.01$.

mainly located in the cytoplasm instead of the nucleus of BCa cells (Fig. 3A-3B). Given that cytoplasmic lncRNAs affect post-transcriptional regulations such as mRNA stability and translational regulation, largely through the competing endogenous RNA (ceRNA) regulation mechanism of adsorbed miRNA [18], HEIH was likely to have the potential of post-transcriptional regulation in BCa. Next, we performed Ago2-RIP assay to verify this hypothesis since the RNA-binding protein (RBP) Ago2 is a key component of the RNA-induced silencing complex

(RISC) and exerts vital functions in global alterations of miRNA levels and activity in the cytoplasm [19]. Ago2-RIP assay indicated that HEIH was highly enriched in Ago2-containing beads (Fig. 3C), verifying the potential of HEIH in ceRNA regulatory network. Thus, we conjectured that HEIH might regulate c-Myc via sponging some specific miR-NAs. However, no mutual miRNA was observed to combine with HEIH and c-Myc (Fig. 3D). Hence, the starBase (https://starbase.sysu.edu.cn) database analysis was carried out to predict HEIH-interacting
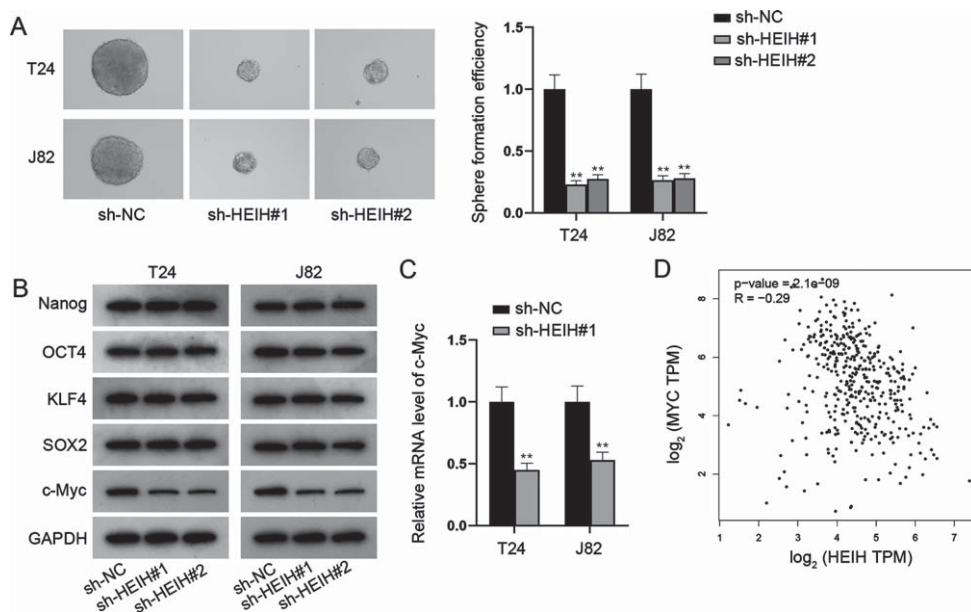
Fig. 2. HEIH contributes to BCa cell stemness via up-regulating c-Myc. (A) Sphere formation assay was performed to evaluate cell stemness in HEIH-silenced BCa cells. (B) Western blot was used to analyze the protein levels of Nanog, OCT4, KLF4, SOX2 and c-Myc in HEIH-inhibited BCa cells. (C) RT-qPCR was used to measure c-Myc mRNA level in HEIH-silenced BCa cells. (D) The correlation of HEIH and MYC expression in BLCA based on GEPIA analysis. **$P < 0.01$.

miRNAs. We discovered 13 miRNAs containing the putative binding sites with HEIH under the threshold of CLIP Data $>= 3$. To certify the binding between candidate miRNAs and HEIH, RNA pull down assays were implemented and showed that only miR-4500 was pulled down by biotinylated HEIH (Bio-HEIH) probe among candidate miRNAs (Fig. 3E). RT-qPCR analysis further demonstrated that miR-4500 was low-expressed in BCa cell lines compared with SV-HUC-1 cell line (Fig. 3F). To explore the function of miR-4500 in BCa progression, we overexpressed miR-4500 in T24 and J82 cells (Fig. S1A), and found that enforced expression of miR-4500 impeded cell proliferation, migration, invasion and stemness while promoted cell apoptosis in BCa (Fig. S1B-S1H). Moreover, we found that HEIH was pulled down by biotin-labeled miR-4500 wild-type (Bio-miR-4500-WT) instead of mutant-type (Bio-miR-4500-Mut; Fig. 3G). The binding sites of HEIH and miR-4500 were disclosed in Fig. 3H, and luciferase reporter assays further showed that the luciferase activity of HEIH wild-type (HEIH-WT) was repressed by miR-4500 mimics, whereas that of HEIH mutant-type (HEIH-Mut) was barely influenced (Fig. 3I). Altogether, HEIH acts as a miR-4500 sponge in BCa cells, and miR-4500 plays a suppressive role in BCa.

HEIH sponges miR-4500 to regulate IGF2BP1

With the help of bioinformatics, 9 mRNAs were predicted to be targeted by miR-4500 (Fig. 4A). Through RT-qPCR analysis, we found that only IGF2BP1 was markedly down-regulated in miR-4500-overexpressed BCa cells (Fig. 4B). Besides, we found that IGF2BP1 was expressed at a higher level in BCa cell lines versus SV-HUC-1 cell line (Fig. 4C). RIP assays showed that HEIH, miR-4500 and IGF2BP1 were abundant in Ago2 precipitates (Fig. 4D), further validating the interaction of these three RNAs. Besides, RNA pull down assays uncovered that IGF2BP1 was preferentially abundant in Bio-miR-4500-WT group while Bio-miR-4500-Mut group had no marked change versus control (Fig. 4E). Moreover, we discovered the binding sites of IGF2BP1 3'UTR and miR-4500 (Fig. 4F). Luciferase reporter assay indicated that miR-4500 elevation markedly declined the luciferase activities of IGF2BP1 3'UTR-WT while IGF2BP1 3'UTR-Mut had no marked change in luciferase activities (Fig. 4G). In addition, we found that HEIH deficiency obviously reduced IGF2BP1 mRNA and protein levels while this was abrogated after simultaneous miR-4500 inhibition (Fig. 4H). Meanwhile, we found that IGF2BP1 mRNA and c-Myc protein levels were
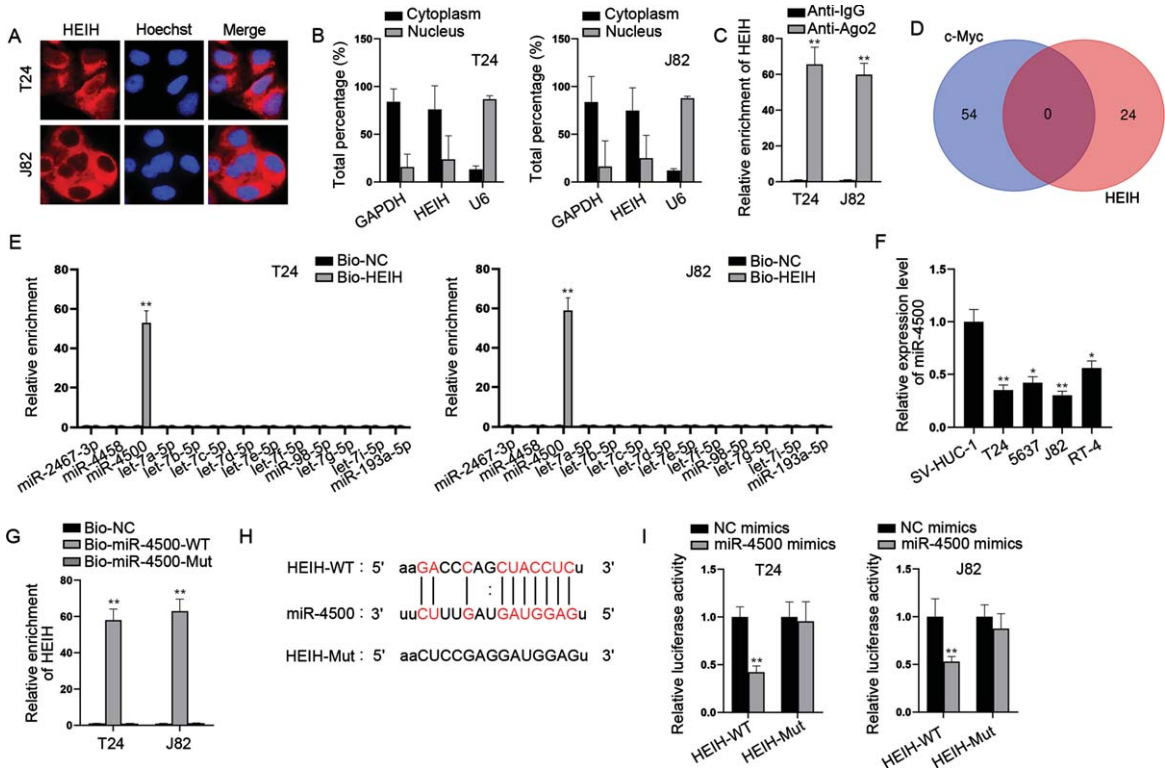
Fig. 3. HEIH sponges miR-4500 in BCa cells. (A-B) Cellular position of HEIH was certified by FISH and subcellular fractionation assays. (C) RIP experiment detected the existence of HEIH in Ago2-RISC. (D) Venn diagram illustrated no shared miRNAs bound to HEIH and c-Myc. (E) RNA pull down assay detected the combination between HEIH and candidate miRNAs. (F) Expression of miR-4500 in BCa cells was detected via RT-qPCR. (G) RNA pull down experiment tested the abundance of HEIH in biotinylated miR-4500-WT or miR-4500-Mut. (H) The binding sites of miR-4500 and HEIH. (I) Luciferase activity of HEIH-WT and HEIH-Mut in BCa cells after miR-4500 overexpression was detected. $^{*}P < 0.05$, $^{**}P < 0.01$.

increased by miR-4500 inhibition alone (Fig. 4H). Taken together, HEIH sponges miR-4500 to upregulate IGF2BP1 expression in BCa cells.

HEIH regulates c-Myc expression via targeting the miR-4500/IGF2BP1 axis

Previous literatures have indicated that IGF2BP1 can bind to and stabilize c-Myc mRNA [20]. Thus, we hypothesized that HEIH might regulate c-Myc expression via targeting the miR-4500/IGF2BP1 axis. Herein, we first detected the binding between IGF2BP1 and c-Myc in BCa (Fig. 5A). Then, we silenced IGF2BP1 expression in BCa cells (Fig. 5B), and found that knockdown of IGF2BP1 significantly repressed c-Myc expression at mRNA and protein levels (Fig. 5C). Moreover, after treatment with Actinomycin D, the stability of c-Myc mRNA was restrained when HEIH or IGF2BP1 was down-regulated (Fig. 5D). In addition, to determine whether HEIH promotes BCa cell growth and

stemness via regulating c-Myc, we overexpressed c-Myc expression in BCa cells (Fig. S2A), and then severally transfected sh-NC, sh-HEIH#1, sh-HEIH#1 + pcDNA3.1/c-Myc into cells to perform rescue experiments. It was found that overexpression of c-Myc offset the inhibited proliferation of HEIH-silenced cells (Fig. S2B-S2C). Besides, the enhanced apoptosis induced by HEIH depletion was countervailed by c-Myc overexpression (Fig. S2D-2E). Moreover, we observed that the reduced migration, invasion and sphere-forming ability caused by HEIH deficiency were counteracted by synchronous c-Myc elevation (Fig. S2F-S2H). To sum up, HEIH regulates c-Myc expression via targeting the miR-4500/IGF2BP1 axis.

c-Myc transcriptionally activates HEIH expression

We further explored the upstream mechanism of HEIH in BCa cells. With the help of UCSC (https://
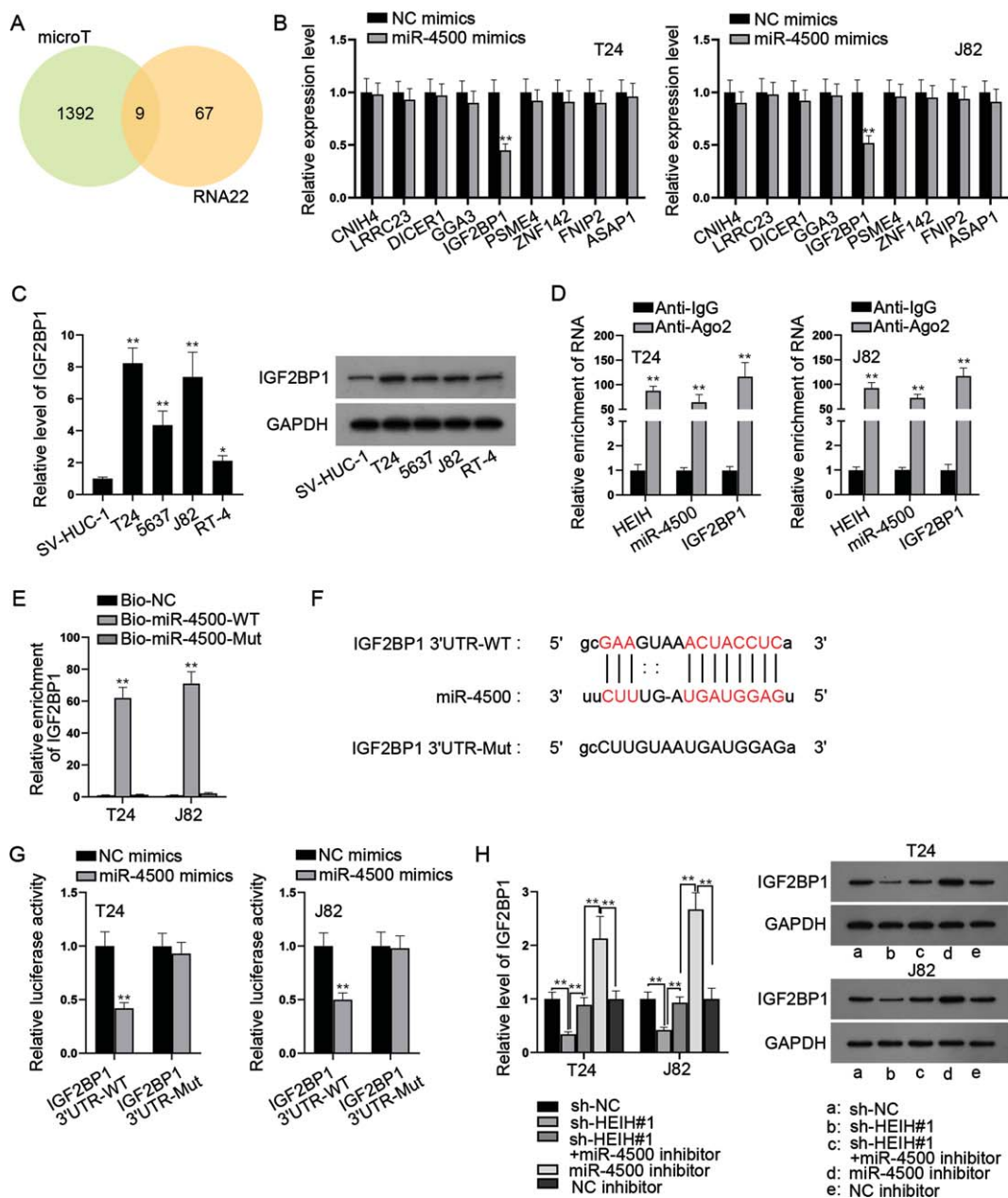
Fig. 4. HEIH sponges miR-4500 to regulate IGF2BP1. (A) Venn diagram showed 9 putative target mRNAs of miR-4500 predicted by microT and RNA22 algorithms. (B) RT-qPCR was used to analyze the expression of 9 mRNAs in miR-4500-overexpressed BCa cells. (C) RT-qPCR and western blot were applied to measure IGF2BP1 expression in BCa cell lines and SV-HUC-1 cell line. (D) RIP assays were performed to detect the enrichment of HEIH, miR-4500 and IGF2BP1 in Ago2-bound precipitates. (E) RNA pull down assays were conducted to detect the abundance of IGF2BP1 in Bio-miR-4500-WT group and Bio-miR-4500-Mut group. (F) Binding sites of IGF2BP1 3'UTR and miR-4500 and mutated sequence of IGF2BP1 3'UTR-Mut. (G) Luciferase activity of IGF2BP1 3'UTR-WT and IGF2BP1 3'UTR-Mut was detected in BCa cells co-transfected with miR-4500 mimics. (H) IGF2BP1 mRNA and protein levels in BCa cells transfected with sh-NC, sh-HEIH#1, sh-HEIH#1 + miR-4500 inhibitor, miR-4500 inhibitor or NC inhibitor using RT-qPCR and western blot. $*P < 0.05$, $**P < 0.01$.

genome.ucsc.edu/) and JASPAR (https://jaspar. genereg.net/) databases, we discovered that c-Myc was a transcription factor that binds to the promoter region of HEIH (Fig. 6A-6B). Subsequently, c-Myc

was knocked down in BCa cells and the knockdown efficiency of sh-c-Myc was verified by RT-qPCR and western blot analyses (Fig. 6C). We found that HEIH expression was restrained in c-Myc-depleted
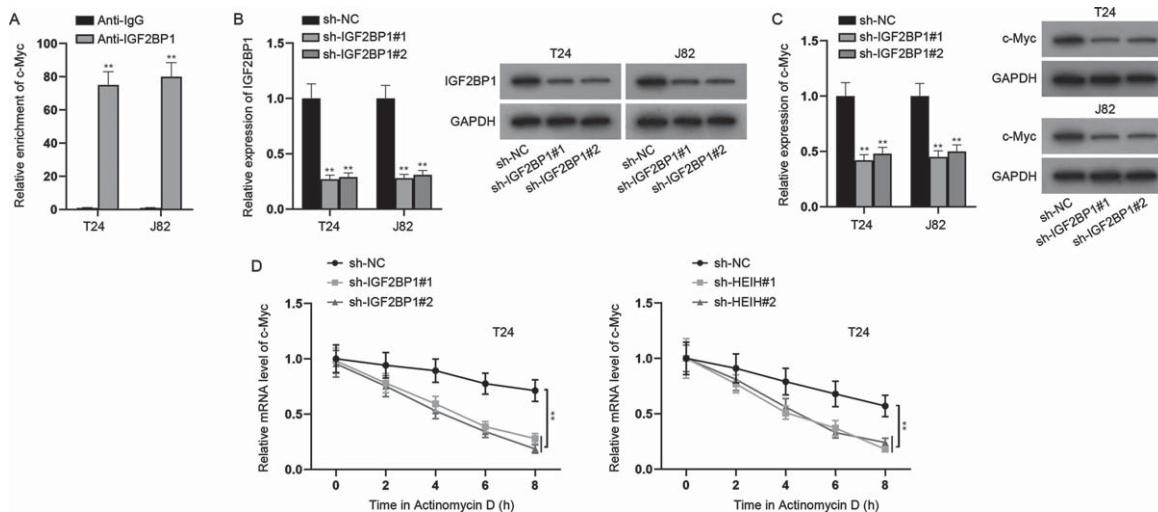
Fig. 5. HEIH regulates c-Myc expression via targeting the miR-4500/IGF2BP1 axis. (A) ChIP assays were performed to detect the combination between c-Myc and IGF2BP1 in BCa cells. (B) Silencing efficiency of IGF2BP1 in BCa cells was verified by RT-qPCR and western blot. (C) RT-qPCR and western blot were used to detect c-Myc mRNA and protein levels in IGF2BP1-silenced BCa cells. (D) Stability of c-Myc mRNA was detected in IGF2BP1-silenced or HEIH-depleted BCa cells after Actinomycin D treatment. $**P < 0.01$.

BCa cells (Fig. 6D). Further, ChIP assay showed that HEIH promoter was highly expressed in the complexes precipitated by anti-c-Myc versus control anti-IgG (Fig. 6E), suggesting the direct binding of c-Myc and HEIH promoter. Similarly, luciferase reporter assay showed that c-Myc suppression significantly weakened the luciferase activity of HEIH promoter-WT instead of that of HEIH promoter-Mut (Fig. 6F). In conclusion, c-Myc activates HEIH expression at the transcriptional level.

HEIH promotes the tumorgenesis and metastasis of BCa in vivo

In addition to *in vitro* assays, we investigated the effect of silenced HEIH on the tumorigenesis and metastasis of BCa. As displayed in Fig. S3A, the size of tumors in the sh-HEIH#1 group was significantly smaller than that in the sh-NC group. Tumor volume and weight were also reduced in HEIH-depleted group versus sh-NC group (Fig. S3B). The above results indicated that HEIH knockdown inhibits the tumorgenesis of BCa *in vivo*. Based on the IHC analysis, the expression of the proliferative maker protein PCNA was overtly reduced in the sh-HEIH#1 group versus control (Fig. S3C), indicating that HEIH silencing hampers tumor growth *in vivo*. Additionally, H&E staining was performed to evaluate lung metastasis. The number of lung metastatic nodules was sharply decreased in HEIH-ablated group versus control (Fig. S3D), suggesting that HEIH inhibition

represses the metastasis of BCa *in vivo*. Altogether, HEIH facilitates the tumorgenesis and metastasis of BCa *in vivo*.

DISCUSSION

Our study, for the first time, demonstrated that HEIH was highly expressed in BCa cell lines and clarified its role in BCa. Functionally, depleted HEIH inhibits BCa cell proliferation, migration, invasion while elevates cell apoptosis, suggesting that HEIH might exert an oncogenic role in BCa progression. This is in line with findings reported in previous studies that HEIH functions as a tumor facilitator in a variety of human cancers. For example, HEIH enhances cell proliferation and suppresses apoptosis in triple-negative breast cancer [21]. HEIH promotes liver cancer cell growth and metastasis [22]. HEIH facilitates the tumorigenesis of colorectal cancer [23].

Our study also revealed that HEIH induces BCa cell stemness via up-regulating c-Myc. CSCs play a vital role in the progression of malignant tumors, including BCa. Notably, c-Myc is one of the most frequently activated oncogenes in the development of human cancers, including BCa [24–26]. Besides, c-Myc has been considered as a crucial modulator of stem cell biology [27]. Mounting evidences have shown that c-Myc can regulate the stemness of various cancer cells [28, 29]. Thus, targeting c-Myc may be a promising strategy for cancer therapy.
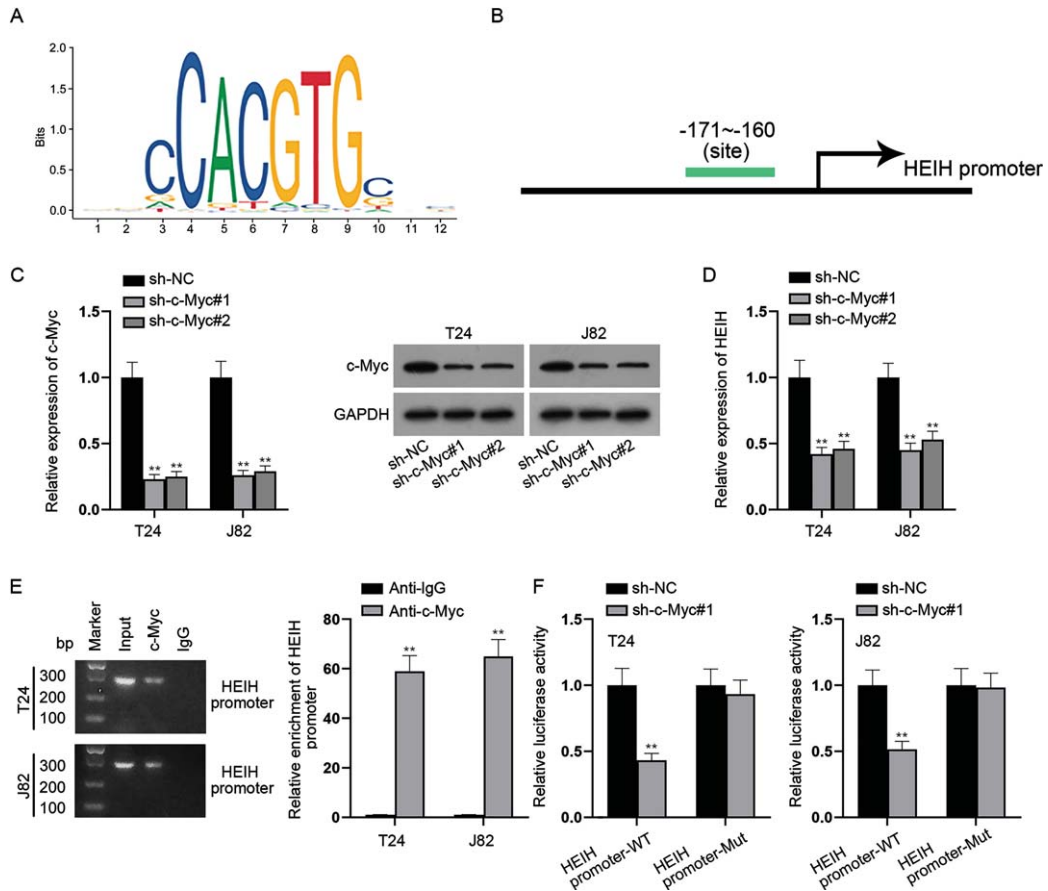
Fig. 6. c-Myc transcriptionally activates HEIH expression. (A-B) UCSC and JASPAR databases predicted the c-Myc-binding sites (−171∼−160) in the sequence of HEIH promoter region. (C) Silencing efficiency of c-Myc in BCa cells was validated using RT-qPCR and western blot. (D) HEIH expression in c-Myc-depleted BCa cells was detected by RT-qPCR. (E) Combination between HEIH promoter and c-Myc in BCa cells was examined by ChIP assay. DNA bands were visualized using agarose gel electrophoresis (left panel). Quantification of HEIH promoter by RT-qPCR after ChIP was shown (right panel). (F) Luciferase activity of HEIH promoter-WT and HEIH promoter-Mut was detected in BCa cells after c-Myc deficiency. **$P < 0.01$.

A further finding of our study was that HEIH acts as a ceRNA of miR-4500 in BCa cells. This ceRNA mechanism was in line with previous studies on HEIH regulation in cancers. For instance, HEIH has been reported to suppress hepatocellular carcinoma cell growth by interacting with miR-199a-3p [30]. Lei Jiang et al. have pointed that HEIH contributes to gastric carcinoma cell proliferation, migration and invasion by targeting miR-214-3p [31]. Moreover, miR-4500 has been reported to exert a suppressive function in multiple human cancers. MiR-4500 hinders papillary thyroid cancer progression via modulating PLXNC1 [32]. MiR-4500 represses non-small cell lung cancer progression by affecting STAT3 [33]. MiR-4500 impedes breast cancer cell migration and invasion via targeting RRM2 [34]. Consistently, miR-4500 was proved to be poorly expressed in BCa

cells, and we found that overexpression of miR-4500 inhibits BCa progression. Moreover, our study demonstrated that HEIH sponges miR-4500 to up-regulate IGF2BP1 expression.

IGF2BP1 as a RBP has been reported to regulate the stability of mRNAs, such as PEG10 [35], ELF3 [36] and SOX2 [37]. Of note, IGF2BP1 is well-known to maintain the stability of c-Myc mRNA [38]. Herein, our study further uncovered that HEIH up-regulates c-Myc via targeting the miR-4500/IGF2BP1 axis in BCa cells. Additionally, mounting studies have identified that c-Myc can activate multiple lncRNAs, such as NEAT1 [39], LINC01123 [40] and FGF13-AS1 [41] via transcriptional regulation. Herein, c-Myc was verified to act as a transcriptional factor to activate HEIH expression in BCa.

Moreover, the current study validated the promoting effect of HEIH on the tumorgenesis and metastasis of BCa through *in vivo* experiments. However, this study lacked the clinicopathological analysis. In the further exploration, we will investigate the correlation between HEIH expression and clinicopathological features of BCa patients.

In conclusion, our study revealed that HEIH, highly expressed in BCa cell lines, functions as an oncogene by facilitating cell proliferation, migration and invasion as well as stemness. Our findings demonstrated that HEIH expression and c-Myc activation forms a positive feedback loop to control BCa progression by targeting miR-4500 to up-regulate IGF2BP1 expression, which might offer novel insight into BCa treatment.

ACKNOWLEDGMENTS

FUNDING

AUTHOR CONTRIBUTIONS

Baowei Guo: writing the article
Dan Zhao: conception
Jiao Feng: performance of work
Yanmei Liu: interpretation of data.

ETHICAL CONSIDERATIONS

Animal study was approved by the Yidu Central Hospital of Weifang.

CONFLICT OF INTEREST

Baowei Guo has no conflict of interest to report.
Dan Zhao has no conflict of interest to report.
Jiao Feng has no conflict of interest to report.
Yanmei Liu has no conflict of interest to report.

REFERENCES

[1] Grayson M. Bladder cancer. Nature. 2017;551(7679):S33.

[2] Berdik C. Unlocking bladder cancer. Nature. 2017;551 (7679):S34-s5.

[3] Kirkali Z, Chan T, Manoharan M, Algaba F, Busch C, Cheng L, et al. Bladder cancer: epidemiology, staging and grading, and diagnosis. Urology. 2005;66(6 Suppl 1):4-34.

[4] Farling KB. Bladder cancer: Risk factors, diagnosis, and management. The Nurse Practitioner. 2017;42(3):26-33.

[5] Huang R, Rofstad EK. Cancer stem cells (CSCs), cervical CSCs and targeted therapies. Oncotarget. 2017;8(21): 35351-67.

[6] Li Y, Lin K, Yang Z, Han N, Quan X, Guo X, et al. Bladder cancer stem cells: clonal origin and therapeutic perspectives. Oncotarget. 2017;8(39):66668-79.

[7] Chan JJ, Tay Y. Noncoding RNA:RNA Regulatory Networks in Cancer. International Journal of Molecular Sciences. 2018;19(5).

[8] Sharma H, Carninci P. The Secret Life of lncRNAs: Conserved, yet Not Conserved. Cell. 2020;181(3):512-4.

[9] Huang X, Zhi X, Gao Y, Ta N, Jiang H, Zheng J. LncRNAs in pancreatic cancer. Oncotarget. 2016;7(35):57379-90.

[10] Chen C, He W, Huang J, Wang B, Li H, Cai Q, et al. LNMAT1 promotes lymphatic metastasis of bladder cancer via CCL2 dependent macrophage recruitment. Nature Communications. 2018;9(1):3826.

[11] Tuo Z, Zhang J, Xue W. LncRNA TP73-AS1 predicts the prognosis of bladder cancer patients and functions as a suppressor for bladder cancer by EMT pathway. Biochemical and Biophysical Research Communications. 2018;499(4): 875-81.

[12] Zhang R, Wang J, Jia E, Zhang J, Liu N, Chi C. lncRNA BCAR4 sponges miR-370-3p to promote bladder cancer progression via Wnt signaling. International Journal of Molecular Medicine. 2020;45(2):578-88.

[13] Ding X, Qi C, Min J, Xu Z, Huang K, Tang H. Long non-coding RNA HEIH suppresses the expression of TP53 through enhancer of zeste homolog 2 in oesophageal squamous cell carcinoma. Journal of Cellular and Molecular Medicine. 2020;24(18):10551-9.

[14] Han YE, Tao JM, Wang SX, Ju X, Song ZY. Long non-coding RNA HEIH modulates CDK8 expression by inhibiting miR-193a-5p to accelerate nasopharyngeal carcinoma progression. European Review for Medical and Pharmacological Sciences. 2021;25(2):770-8.

[15] Liu G, Guo W, Chen G, Li W, Cui Y, Qin J, et al. Lnc-MCEI mediated the chemosensitivity of esophageal squamous cell carcinoma via miR-6759-5p to competitively regulate IGF2. International Journal of Biological Sciences. 2020;16(15):2938-50.

[16] Suo D, Wang Z, Li L, Chen Q, Zeng T, Liu R, et al. HOXC10 upregulation confers resistance to chemoradiotherapy in ESCC tumor cells and predicts poor prognosis. Oncogene. 2020;39(32):5441-54.

[17] Si L, Chen J, Yang S, Liu Z, Chen Y, Peng M, et al. lncRNA HEIH accelerates cell proliferation and inhibits cell senescence by targeting miR-3619-5p/CTTNBP2 axis in ovarian cancer. Menopause (New York, NY). 2020;27(11):1302-14.

[18] Cao Z, Pan X, Yang Y, Huang Y, Shen HB. The lncLocator: a subcellular localization predictor for long non-coding RNAs based on a stacked ensemble classifier. Bioinformatics (Oxford, England). 2018;34(13):2185-94.

[19] Tarallo R, Giurato G, Bruno G, Ravo M, Rizzo F, Salvati A, et al. The nuclear receptor ERβ engages AGO2 in regulation of gene transcription, RNA splicing and RISC loading. Genome Biology. 2017;18(1):189.

[20] Zhu S, Wang JZ, Chen D, He YT, Meng N, Chen M, et al. An oncopeptide regulates m(6)A recognition by the m(6)A reader IGF2BP1 and tumorigenesis. Nature Communications. 2020;11(1):1685.

[21] Li Z, Qin X, Bian W, Li Y, Shan B, Yao Z, et al. Exosomal lncRNA ZFAS1 regulates esophageal squamous

cell carcinoma cell proliferation, invasion, migration and apoptosis via microRNA-124/STAT3 axis. Journal of Experimental & Clinical Cancer Research : CR. 2019;38(1):477.

[22] Ma Y, Cao D, Li G, Hu J, Liu X, Liu J. Silence of lncRNA HEIH suppressed liver cancer cell growth and metastasis through miR-199a-3p/mTOR axis. Journal of Cellular Biochemistry. 2019;120(10):17757-66.

[23] Cui C, Zhai D, Cai L, Duan Q, Xie L, Yu J. Long Noncoding RNA HEIH Promotes Colorectal Cancer Tumorigenesis via Counteracting miR-939-Mediated Transcriptional Repression of Bcl-xL. Cancer Research and Treatment : Official Journal of Korean Cancer Association. 2018;50(3):992-1008.

[24] Sun J, Zhang H, Tao D, Xie F, Liu F, Gu C, et al. Circ-CDYL inhibits the expression of C-MYC to suppress cell growth and migration in bladder cancer. Artificial cells, Nanomedicine, and Biotechnology. 2019;47(1):1349-56.

[25] Wang J, Zhao X, Shi J, Pan Y, Chen Q, Leng P, et al. miR-451 suppresses bladder cancer cell migration and invasion via directly targeting c-Myc. Oncology Reports. 2016;36(4):2049-58.

[26] Liu B, Gao W, Sun W, Li L, Wang C, Yang X, et al. Promoting roles of long non-coding RNA FAM83H-AS1 in bladder cancer growth, metastasis, and angiogenesis through the c-Myc-mediated ULK3 upregulation. Cell Cycle (Georgetown, Tex). 2020;19(24):3546-62.

[27] Yoshida GJ. Emerging roles of Myc in stem cell biology and novel tumor therapies. Journal of Experimental & Clinical Cancer Research : CR. 2018;37(1):173.

[28] Zhang L, Ma R, Gao M, Zhao Y, Lv X, Zhu W, et al. SNORA72 Activates the Notch1/c-Myc Pathway to Promote Stemness Transformation of Ovarian Cancer Cells. Frontiers in Cell and Developmental Biology. 2020;8:583087.

[29] Gao X, Liu X, Lu Y, Wang Y, Cao W, Liu X, et al. PIM1 is responsible for IL-6-induced breast cancer cell EMT and stemness via c-myc activation. Breast Cancer (Tokyo, Japan). 2019;26(5):663-71.

[30] Wu MM, Shen WD, Zou CW, Chen HJ, Guo HM. LncRNA-HEIH suppresses hepatocellular carcinoma cell growth and metastasis by up-regulating miR-199a-3p. European Review for Medical and Pharmacological Sciences. 2020;24(11):6031-8.

[31] Jiang L, Zhang L, Chen Q, Qiao S, Zhou F, Han M. LncRNA HEIH promotes cell proliferation, migration and invasion by suppressing miR-214-3p in gastric carcinoma. Journal of Biochemistry. 2020.

[32] Li R, Teng X, Zhu H, Han T, Liu Q. MiR-4500 Regulates PLXNC1 and Inhibits Papillary Thyroid Cancer Progression. Hormones & Cancer. 2019;10(4-6):150-60.

[33] Li ZY, Zhang ZZ, Bi H, Zhang QD, Zhang SJ, Zhou L, et al. MicroRNA-4500 suppresses tumor progression in non-small cell lung cancer by regulating STAT3. Molecular Medicine Reports. 2019;20(6):4973-83.

[34] Li S, Mai H, Zhu Y, Li G, Sun J, Li G, et al. MicroRNA-4500 Inhibits Migration, Invasion, and Angiogenesis of Breast Cancer Cells via RRM2-Dependent MAPK Signaling Pathway. Molecular Therapy Nucleic Acids. 2020;21:278-89.

[35] Zhang L, Wan Y, Zhang Z, Jiang Y, Gu Z, Ma X, et al. IGF2BP1 overexpression stabilizes PEG10 mRNA in an m6A-dependent manner and promotes endometrial cancer progression. Theranostics. 2021;11(3):1100-14.

[36] Feng Y, Gao L, Cui G, Cao Y. LncRNA NEAT1 facilitates pancreatic cancer growth and metastasis through stabilizing ELF3 mRNA. American Journal of Cancer Research. 2020;10(1):237-48.

[37] Xue T, Liu X, Zhang M, E Q, Liu S, Zou M, et al. PADI2-Catalyzed MEK1 Citrullination Activates ERK1/2 and Promotes IGF2BP1-Mediated SOX2 mRNA Stability in Endometrial Cancer. Advanced science (Weinheim, Baden-Wurttemberg, Germany). 2021;8(6):2002831.

[38] Zhu P, He F, Hou Y, Tu G, Li Q, Jin T, et al. A novel hypoxic long noncoding RNA KB-1980E6.3 maintains breast cancer stem cell stemness via interacting with IGF2BP1 to facilitate c-Myc mRNA stability. Oncogene. 2021;40(9):1609-27.

[39] Zeng C, Liu S, Lu S, Yu X, Lai J, Wu Y, et al. The c-Myc-regulated lncRNA NEAT1 and paraspeckles modulate imatinib-induced apoptosis in CML cells. Molecular Cancer. 2018;17(1):130.

[40] Hua Q, Jin M, Mi B, Xu F, Li T, Zhao L, et al. LINC01123, a c-Myc-activated long non-coding RNA, promotes proliferation and aerobic glycolysis of non-small cell lung cancer through miR-199a-5p/c-Myc axis. Journal of hematology & oncology. 2019;12(1):91.

[41] Ma F, Liu X, Zhou S, Li W, Liu C, Chadwick M, et al. Long non-coding RNA FGF13-AS1 inhibits glycolysis and stemness properties of breast cancer cells through FGF13-AS1/IGF2BPs/Myc feedback loop. Cancer Letters. 2019;450:63-75.